

Aspects of classical and quantum motion on a flux cone ¹

E. S. Moreira Jnr.²

*Instituto de Física Teórica
Universidade Estadual Paulista,
Rua Pamplona, 145
01405-900 - São Paulo, S.P., Brazil*

August, 1997

Abstract

Motion of a non-relativistic particle on a cone with a magnetic flux running through the cone axis (a “flux cone”) is studied. It is expressed as the motion of a particle moving on the Euclidean plane under the action of a velocity-dependent force. Probability fluid (“quantum flow”) associated with a particular stationary state is studied close to the singularity, demonstrating non trivial Aharonov-Bohm effects. For example, it is shown that near the singularity quantum flow departs from classical flow. In the context of the hydrodynamical approach to quantum mechanics, quantum potential due to the conical singularity is determined and the way it affects quantum flow is analysed. It is shown that the winding number of classical orbits plays a role in the description of the quantum flow. Connectivity of the configuration space is also discussed.

1 Introduction

Usually, when the quantum description of a system is non trivial, so is the classical one. However this is not always the case. There is a number of examples whose intrinsic quantum effects do not have a classical analogue. Notable among these is the Aharonov-Bohm (A-B) effect [1]. In this set up, the magnetic field vanishes everywhere except inside a thin flux tube. As there is no Lorentz force, classically particles are free, and are not affected

¹Work supported by FAPESP grant 96/12259-1.

²e-mail: moreira@axp.ift.unesp.br

by the background. However in the quantum scattering problem the background leads to a non trivial scattering, which is confirmed by experiment [2]. A curious fact about the A-B effect is that by choosing an appropriate gauge the quantum mechanical equations of motion become free equations and the interaction of quantum matter with a singular vector potential becomes encoded in unconventional boundary conditions.

The A-B effect is a consequence of the interaction of quantum matter with a *nearly* trivial affine connection and it is present in every gauge theory, including gravity. The analogue of the A-B set up in gravitation is a conical background [3, 4, 5]. The geometry is flat everywhere apart from a symmetry axis. As in the case of a thin flux tube, the problem of studying quantum theory in this background amounts to solving the usual equations in flat space, with the non trivial conical geometry manifested only in the boundary conditions. Solutions of these equations lead to geometrical Aharonov-Bohm effects. It should be remarked that there is an important distinction between A-B effects in ordinary gauge theories and those in gravity. In ordinary gauge theories, matter does not couple with (non trivial) connections in the classical equations of motion but with (vanishing) field strengths. This is not the case in gravity where (non trivial) connections are also present in the classical equations of motion, making the effect appear even in the classical theory. An interesting example is the self-force induced by conical singularities [6, 7]. Another is the double images effect due to cosmic strings, whose external gravitational field may approximately be described by a conical geometry [8].

Quantum theory on cones has been studied over two decades [9], and investigations intensified in the mid-eighties [7, 10] very much due to the importance in cosmology of cosmic strings. More recently interest in the subject was renewed in the context of quantum mechanics of black holes, where one encounters conical singularities (see e.g. [11] and references therein). Besides these and other practical motivations to study quantum theory in conical backgrounds, there is another more academic one [12-14]. Namely, the study of quantum mechanics in a *nearly* trivial gravitational background may shed some light on the profound problems of combining quantum mechanics and general relativity.

In this work classical and quantum effects caused by a conical singularity on the motion of a particle are studied. On various occasions the A-B set up is coupled to a conical geometry (flux cone), so that a detailed comparison of the corresponding A-B effects is possible. The paper is organized as follows. A study of the conical geometry is given in section 2, commenting on points which have been overlooked in the literature. In particular the Aharonov-Bohm like features of the Levi-Civita connection are stressed. A regularization method of determining the localized curvature of a cone is proposed. Positive and negative deficit angles are considered and related with the curvature. The relevant coordinate systems are defined. In section 3 classical motion on a flux cone is studied. The effects of the conical singularity are shown to be equivalent to the ones due to an angular momentum dependent force. In section 4 quantization is implemented by the usual substitution principle. The issue of boundary conditions at the singularity is considered, and a particular one is chosen, motivated by regularization arguments given in [15, 16]. Corresponding stationary states are obtained and used to build up a state to probe the singularity. This leads, in section 5, to the study of quantum flow, showing new

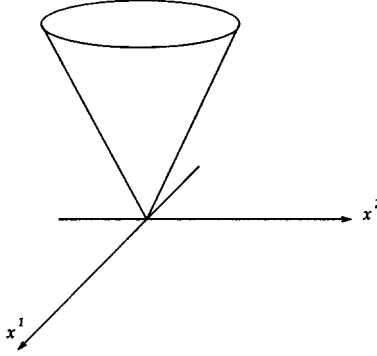


Figure 1: Cone embedded in a 3-dimensional Euclidean space.

non trivial effects due to the conical singularity. Such effects are caused by a non vanishing quantum potential whose features are mentioned. Connectivity of the configuration space is discussed by taking into account the behaviour of quantum flow at the singularity. The last section is a summary, including possible extensions of this study. An account on the hydrodynamical approach to quantum mechanics (whose elements are used in section 5) is given in the appendix.

2 The cone

A cone is a 2-dimensional space with a δ -function curvature singularity. The curvature tensor is concentrated at a single point, vanishing everywhere else [17]. The line element may be written as

$$\begin{aligned} dl^2 &= g_{ij} dx^i dx^j \\ &= \left[\delta_{ij} + (\alpha^{-2} - 1) \frac{x^i x^j}{r^2} \right] dx^i dx^j, \end{aligned} \quad (1)$$

where the coordinate x^i ($i = 1, 2$) runs from $-\infty$ to ∞ , $r^2 := \delta_{ij} x^i x^j$ and α is a positive parameter [18]. Imagining the conical surface embedded in a 3-dimensional Euclidean space, $\{x^1, x^2\}$ are Cartesian coordinates on a plane perpendicular to the symmetry axis of the cone (Fig. 1). From (1) one sees that the conical singularity is located at the origin and that when $\alpha = 1$ the cone becomes the Euclidean plane.

Using polar coordinates ($x^1 = r \cos \theta$, $x^2 = r \sin \theta$), the line element (1) can be rewritten as $dl^2 = \alpha^{-2} dr^2 + r^2 d\theta^2$ where the conical singularity is now hidden by the coordinate singularity at the origin, since the polar angle θ is not defined at $r = 0$. Note that the coordinates (r, θ) and $(r, \theta + 2\pi)$ label the same point, $(r, \theta) \sim (r, \theta + 2\pi)$. A further simplification of the line element can be made by rescaling $\{r, \theta\}$ as

$$\rho = \alpha^{-1} r \quad \varphi = \alpha \theta, \quad (2)$$

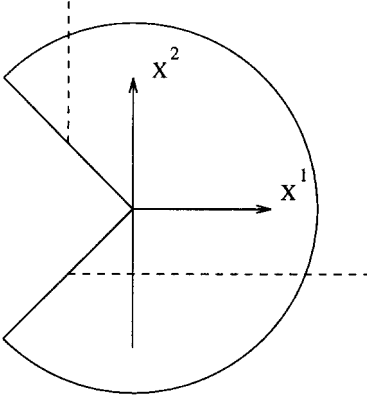


Figure 2: Singular Cartesian frame.

resulting in

$$dl^2 = d\rho^2 + \rho^2 d\varphi^2, \quad (3)$$

which is the line element of the Euclidean plane written in polar coordinates, showing the flatness of the cone. However, as a consequence of the rescaling, now the coordinates (ρ, φ) and $(\rho, \varphi + 2\pi\alpha)$ label the same point,

$$(\rho, \varphi) \sim (\rho, \varphi + 2\pi\alpha). \quad (4)$$

This unusual identification encapsulates the fact that the space is a cone and not the Euclidean plane. The coordinates $\{\rho, \varphi\}$ are polar coordinates on the surface of the cone, and they may be visualized by cutting the cone along its generating line and opening it flat. The angle of the missing wedge (extra wedge, when $\alpha > 1$) is the deficit angle of the cone $\mathcal{D} = 2\pi(1 - \alpha)$ (Fig. 2).

At this point it should be noted that the Euclidean plane and a cone have the same topology, differing in their geometry - the former is globally flat whereas the latter is not. To see this, one smoothes the cone by replacing its tip by a tangential spherical cap of radius a (Fig. 3). Clearly the resulting surface is simply connected, a fact that does not change when $a \rightarrow 0$ and the idealized cone is recovered. As the curvature scalar of the spherical cap is given by $R = -2/a^2$, one is left with a curvature singularity surrounded by a flat surface. By considering the line element on the sphere, it may be easily shown that

$$\int d^2x \sqrt{g} R = -2\mathcal{D}, \quad (5)$$

which demonstrates the delta function character of the conical singularity. Note that though the cone is a simply connected background, the configuration space of a quantum particle living on it may be non simply connected (see section 5).

It follows from (4) that the “Cartesian” coordinates defined by $X^1 := \rho \cos \varphi$ and $X^2 := \rho \sin \varphi$ (Fig. 2) are singular if $\mathcal{D} \neq 0$: in terms of $\{X^1, X^2\}$ the metric tensor is Euclidean everywhere except on the rays defining the borders of the wedge, where these

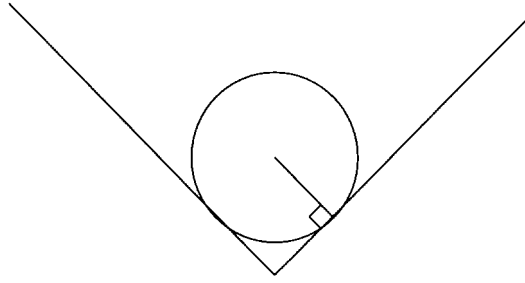


Figure 3: Smoothing the cone.

coordinates are discontinuous functions of φ (In order to obtain the “Euclidean” metric tensor from (3) one has to differentiate a discontinuous function.). The borders of the wedge can be arbitrarily rotated by redefining the interval of length $2\pi\alpha$ over which φ ranges. For example, when $0 \leq \varphi < 2\pi\alpha$ the borders are at $\varphi = 0 \sim 2\pi\alpha$, and at $\varphi = -\pi\alpha \sim \pi\alpha$ when $-\pi\alpha \leq \varphi < \pi\alpha$, which is the case illustrated in Fig. 2.

Corresponding to the behaviour of the metric tensor in terms of $\{X^1, X^2\}$, the Levi-Civita connection vanishes everywhere except on the borders of the wedge where it is singular. It should be stressed that the connection does not vanish everywhere around the singularity in contradiction to what is sometimes claimed. If that were the case, a vector parallelly propagated on a closed loop around the singularity would match itself as the loop is completed [5], which clearly does not happen as long as there is a wedge. The non-vanishing connection tells the rest of the space that there is a curvature singularity at the origin, and this non trivial behaviour is the very one responsible for the geometrical Aharonov-Bohm like effects that will be seen in this work.

It is worth remarking that the rays where the metric tensor is singular come into the problem only if one insists on using the singular Cartesian coordinate system. They are a coordinate singularity. Note that for $\alpha > 1$ more than one singular Cartesian coordinate system is needed to cover the whole cone. In this case there is a “branch cut” leading to a new Cartesian coordinate system in which there is an extra wedge (with corresponding negative deficit angle).

In the following sections, both frames $\{X^1, X^2\}$ and $\{x^1, x^2\}$ will be used to study motion on the cone. It will be clear from the text which frame is used in each situation.

3 Classical motion

The classical motion of a free particle with mass M on a conical surface may be determined from the Lagrangian,

$$\begin{aligned} \mathcal{L} &= \frac{1}{2}M (dl/dt)^2 \\ &= \alpha^{-2} \left[\frac{1}{2}M \dot{\mathbf{x}}^2 - (1 - \alpha^2) \frac{\ell^2}{2Mr^2} \right]. \end{aligned} \quad (6)$$

The line element dl is given by (1), the dot denotes differentiation with respect to the time t , $\mathbf{x} := (x^1, x^2)$ and $\ell := \mathbf{x} \times M\dot{\mathbf{x}}$ is the kinematical angular momentum (note that $\mathbf{a} \times \mathbf{b} := \epsilon_{ij}a^ib^j$). The Euler-Lagrange equations of motion, i.e. the geodesic equations on the cone, follow from (6),

$$M\ddot{\mathbf{x}} = -\left(1 - \alpha^2\right) \frac{\ell^2}{Mr^3} \mathbf{e}_r, \quad (7)$$

where $\mathbf{e}_r := \mathbf{x}/r$. One can regard (7) as the equations of motion of a particle moving on the Euclidean plane under the action of an angular-momentum dependent central force, which is attractive for $\alpha < 1$ (negative curvature) [see (5)] and repulsive for $\alpha > 1$ (positive curvature). Clearly when $\ell = 0$ the motion is radial and uniform.

The geometrical force in (7) has the nature of an inertial force [5, 19]. In fact it ranks somewhere between an inertial force and a Newtonian force. Indeed by changing from $\{x^1, x^2\}$ to $\{X^1, X^2\}$, the force is “gauged away” everywhere, apart from the borders of the wedge which is consistent with the statements in the previous section. Therefore, unless $\alpha = 1$, trajectories crossing these rays are broken straight lines, with uniform motion (dashed line in Fig. 2). For $\alpha > 1$ the particle disappears through the branch cut, continuing into another Cartesian coordinate system. Note that another way of seeing this is to consider (4) and that the Lagrangian may be recast as $\mathcal{L} = M(\dot{\rho}^2 + \rho^2\dot{\varphi}^2)/2$, which is the Lagrangian of a free particle moving on the plane.

It is instructive to describe the classical motion in terms of polar coordinates $\{r, \theta\}$. Integration of (7) gives [14, 19]

$$r^2\dot{\theta} = l \quad \dot{r}^2 + \left(\frac{\alpha l}{r}\right)^2 = (\alpha v)^2,$$

where l and v are constants corresponding to conservation of angular momentum and energy, respectively. A second integration gives

$$(vr)^2 = l^2 + \left[\alpha v^2(t - t_0)\right]^2 \quad l \tan \alpha(\theta - \theta_0) = \alpha v^2(t - t_0), \quad (8)$$

resulting in the orbit equation

$$vr \cos \alpha(\theta - \theta_0) = l. \quad (9)$$

For $l \neq 0$ and choosing $\alpha\theta_0 = \pi/2$, it follows from (8) and (9) that a particle initially at $r = \infty$ and $\theta_i = 0$, traveling say counterclockwise, winds

$$w = [1/2\alpha] \quad (10)$$

times around the minimum radius $r_0 = l/v$, and ends up at $r = \infty$ with $\theta_f = \pi(\alpha^{-1} - 2w)$ ($[x]$ denotes the integral part of x). At r_0 the particle reaches a velocity v which is a maximum for $\alpha < 1$ and a minimum for $\alpha > 1$. For $\alpha > 1/2$ the winding number w vanishes, which is obviously the case when the force in (7) is repulsive ($\alpha > 1$). An unusual feature due to the localized curvature is that θ_f does not depend either on the

asymptotic velocity αv or on the impact parameter $l/\alpha v$. Trajectories of particles with different v and l are parallel to each other (in the sense that the direction of the velocity depends on θ only) as shown in Fig. 4. Note that in terms of $\{X^1, X^2\}$, the particles travel parallel to the X^1 axis with velocity $-v$ before hitting the wedge (see dashed line in Fig. 2).

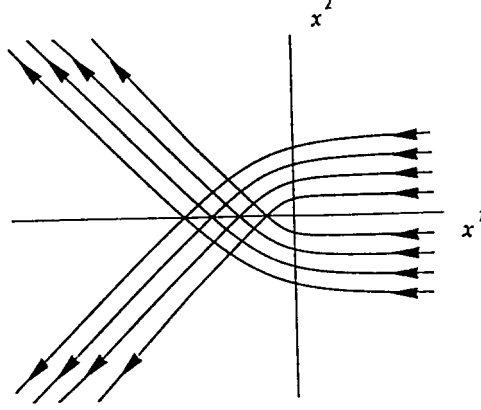


Figure 4: Classical motion on a cone.

A cone may be immersed in a magnetic field pointing along its axis and homogeneous in that direction by choosing a vector potential $\mathbf{A}(\mathbf{x}, t)$ with vanishing component in that direction. The Lagrangian of a particle with charge e moving in this background is given by

$$\mathcal{L}' = \mathcal{L} + \frac{e}{c} \dot{\mathbf{x}} \cdot \mathbf{A}. \quad (11)$$

Thus the canonical momentum associated with \mathbf{x} is

$$\begin{aligned} \mathbf{p} &= \alpha^{-2} \left[M\dot{\mathbf{x}} + \left(\alpha^2 - 1 \right) \frac{\ell}{r} \mathbf{e}_\theta \right] + \frac{e}{c} \mathbf{A} \\ &= M\dot{\mathbf{x}} + \left(\alpha^{-2} - 1 \right) M\dot{r} \mathbf{e}_r + \frac{e}{c} \mathbf{A}. \end{aligned} \quad (12)$$

It follows from (12) that

$$\mathbf{x} \times \mathbf{p} = \ell + \frac{e}{c} \mathbf{x} \times \mathbf{A}, \quad (13)$$

which is the usual expression for the canonical angular momentum on the Euclidean plane. The Hamiltonian is given by

$$\begin{aligned} \mathcal{H} &= \mathbf{p} \cdot \dot{\mathbf{x}} - \mathcal{L}' \\ &= \frac{\alpha^2}{2M} \left(\mathbf{p} - \frac{e}{c} \mathbf{A} \right)^2 + \frac{(1 - \alpha^2)}{2Mr^2} \left[\mathbf{x} \times \left(\mathbf{p} - \frac{e}{c} \mathbf{A} \right) \right]^2. \end{aligned} \quad (14)$$

A magnetic flux $\Phi(t)$ running through the axis of the cone can be introduced by choosing

$$\mathbf{A} = \frac{\Phi}{2\pi r} \mathbf{e}_\theta, \quad (15)$$

where $\mathbf{e}_\theta := (-\sin \theta, \cos \theta)$. Now there is a new singularity at the origin which is a δ -function magnetic field. Due to the cylindrical symmetry, the canonical angular momentum as given by (13) is conserved,

$$\frac{d}{dt} \left(\ell + \frac{e\Phi}{2\pi c} \right) = 0. \quad (16)$$

The equations of motion following from (11) are given by (7), with the induced electric force $-e(\partial_t \Phi) \mathbf{e}_\theta / 2\pi cr$ added on the r.h.s.. This electric force prevents the orbital angular momentum ℓ being a constant of motion, which is consistent with (16). Clearly the above expressions reduce to the familiar ones on the plane [20] when $\alpha = 1$.

The Aharonov-Bohm set up may be combined with the conical geometry by taking Φ constant, in which case the electric force vanishes, and (7) still holds. Obviously the same conclusion may be reached by realizing that the electromagnetic Lagrangian in (11) is a total derivative, $e\Phi\dot{\theta}/2\pi c$, and consequently does not affect classical motion. However, as is well known [1], this is not the case in quantum theory which is the subject of the following sections. (In the following sections, \mathbf{A} is given by (15) with constant Φ .)

4 Hamiltonian operator and stationary states

The Hamiltonian operator H can be obtained from (14) by the usual substitution [14], $\mathbf{p} \rightarrow -i\hbar\nabla$. The invariance of the Schrödinger equation under the gauge transformation $\mathbf{A}(\mathbf{x}) \rightarrow \mathbf{A}(\mathbf{x}) + \nabla\chi(\mathbf{x})$, $\psi(\mathbf{x}, t) \rightarrow \exp\{i(e/\hbar c)\chi(\mathbf{x})\}\psi(\mathbf{x}, t)$ allows the choice $\chi(\mathbf{x}) = (-\Phi/2\pi)\theta(\mathbf{x})$, thereby gauging away the vector potential everywhere, except on an arbitrary ray where the polar angle θ is a discontinuous function of \mathbf{x} [21]. This singular gauge is analogous to the singular Cartesian coordinates $\{X^1, X^2\}$. It might have been anticipated that \mathbf{A} cannot vanish everywhere around the origin since $\oint \mathbf{A} \cdot d\mathbf{x} = \Phi$. Similar reasoning may be applied to the Levi-Civita connection of a conical geometry (see [22] and references therein).

Defining $\sigma := -e\Phi/ch$, the transformed wave function is

$$\psi'(\mathbf{x}, t) = \exp\{i\sigma\theta\}\psi(\mathbf{x}, t). \quad (17)$$

It then follows from (14), (2) and (4) that

$$H = -\frac{\hbar^2}{2M} \frac{1}{\rho} \frac{\partial}{\partial \rho} \left(\rho \frac{\partial}{\partial \rho} \right) + \frac{L^2}{2M\rho^2} \quad (18)$$

$$\psi(\rho, \varphi + 2\pi\alpha) = \exp\{i2\pi\sigma\}\psi(\rho, \varphi), \quad (19)$$

where

$$L := -i\hbar \frac{\partial}{\partial \varphi} \quad (20)$$

and the prime in ψ' has been dropped. As H in (18) is just the free Hamiltonian operator on the plane written in polar coordinates [which is not surprising since $\{X^1, X^2\}$ is a (singular) Cartesian frame], the interaction with the magnetic flux and the conical geometry manifest themselves only through (19). In fact the twisted boundary condition (19) states that the wave function is not single valued, for non integer values of the flux parameter σ , and therefore is not continuous along some ray. This corresponds to (and is compatible with) the fact that H , as given by (18), disguises a singular vector potential which, as mentioned above, is not defined everywhere. Note also that according to (19) ψ must either vanish or diverge at the origin (for non integer σ), otherwise an inconsistency results when a loop is shrunk around $\rho = 0$ [23].

Considering (18) and (19), it follows from the Schrödinger equation

$$\frac{d}{dt} \int_0^\infty d\rho \rho \int_0^{2\pi\alpha} d\varphi \psi \psi^* = \lim_{\rho \rightarrow 0} \int_0^{2\pi\alpha} d\varphi \rho J_\rho, \quad (21)$$

where J_ρ is the usual expression for the radial component of the probability current on the plane,

$$J_\rho = \frac{1}{M} \text{Re} \left[\psi^* \frac{\hbar}{i} \frac{\partial \psi}{\partial \rho} \right] \quad J_\varphi = \frac{1}{M} \text{Re} \left[\psi^* \frac{\hbar}{i\rho} \frac{\partial \psi}{\partial \varphi} \right]. \quad (22)$$

In obtaining (21), it has been assumed that the wave function vanishes at infinity. The r.h.s. of (21) is the net probability crossing an infinitesimally small circle around the singularity. Equating (21) to zero amounts to the statement that the singularity at the origin is neither a source nor a sink (probability is conserved), which is automatically guaranteed if

$$\lim_{\rho \rightarrow 0} \int_0^{2\pi\alpha} d\varphi \rho \left(\psi^* \frac{\partial \phi}{\partial \rho} - \frac{\partial \psi^*}{\partial \rho} \phi \right) = 0. \quad (23)$$

Expression (23) is the condition for self-adjointness of the Hamiltonian operator (18), $\langle \psi | H | \phi \rangle = \langle \phi | H | \psi \rangle^*$.

If $R_{k,m}(\rho)$ are functions such that

$$\left[\rho \frac{\partial}{\partial \rho} \left(\rho \frac{\partial}{\partial \rho} \right) - \left(\frac{m + \sigma}{\alpha} \right)^2 + (k\rho)^2 \right] R_{k,m}(\rho) = 0, \quad (24)$$

then

$$\psi_{k,m}(\rho, \varphi) = \frac{1}{\sqrt{2\pi\alpha}} R_{k,m}(\rho) e^{i(m+\sigma)\varphi/\alpha}, \quad (25)$$

where $0 \leq k < \infty$ and m is an integer, are simultaneous eigenfunctions of H and L with eigenvalues $\hbar^2 k^2 / 2M$ and $(m + \sigma)\hbar / \alpha$, respectively. Note that the effect of the magnetic flux and of the conical geometry on the eigenvalues of L is to shift and to rescale them, respectively. For a particle with spin there is also a shift due to a coupling between the spin and the deficit angle [24, 25].

In order that the stationary states $\psi_{k,m}$ span a space of wave functions in which probability is conserved, they must satisfy (23),

$$\lim_{\rho \rightarrow 0} \rho \left(R_{k',m}^* \frac{\partial R_{k,m}}{\partial \rho} - \frac{\partial R_{k',m}^*}{\partial \rho} R_{k,m} \right) = 0, \quad (26)$$

where the orthonormality relation $\int_0^{2\pi\alpha} d\varphi \exp \{i\varphi(m-n)/\alpha\} = 2\pi\alpha\delta_{mn}$ has been used. Expression (26) is the condition for self-adjointness of the square of the operator $P_\rho := -i\hbar(\partial_\rho + 1/2\rho)$, and is itself self-adjoint if

$$\lim_{\rho \rightarrow 0} \rho (\phi\psi^*) = 0, \quad (27)$$

as may easily be shown by equating $\int_0^\infty d\rho \rho [\phi(P_\rho\psi)^* - \psi^*(P_\rho\phi)]$ to zero. One sees from (27) that $R_{k,m}(\rho)$ may diverge mildly at the origin [which also applies to J_ρ in (21)] and still be compatible with conservation of probability. A mild divergence would not spoil the square integrability of the wave function, since a behavior $\psi \sim 1/\rho^\nu$ with $\nu < 1$ yields $\int_0^\epsilon d\rho \rho |\psi|^2 \propto \epsilon^{2(1-\nu)}$ which vanishes with ϵ . Note that in order to satisfy (27) one must have $\nu < 1/2$. Obviously a logarithmic divergence also passes this test, since it is weaker than the $1/\rho^\nu$ divergence.

In the following only wave functions which are finite at the singularity will be considered. In quantum mechanics on the flux cone, finiteness is motivated by the fact that it arises naturally when the singularities are smoothed by some regularization procedure [15, 16]. [Divergent wave functions have been considered in [15, 16].] Therefore one takes as solutions of (24) Bessel functions of the first kind

$$R_{k,m}(\rho) = J_{|m+\sigma|/\alpha}(k\rho) \quad (28)$$

which being finite at the origin satisfy (27) and consequently (26). As a check we may verify that (28) indeed satisfies (26) by observing that

$$\frac{dJ_\nu(x)}{dx} = \frac{1}{2} [J_{\nu-1}(x) - J_{\nu+1}(x)]. \quad (29)$$

Hence the complete set of stationary states $\psi_{k,m}$ is given by (25) and (28).

A particular state to probe the singularity can be found as follows. The general expression for a stationary state of energy $\hbar^2 k^2/2M$ is given by

$$\psi_k(\rho, \varphi) = \sum_{m=-\infty}^{\infty} c_m \psi_{k,m}(\rho, \varphi). \quad (30)$$

The coefficients c_m are determined by considering the Fourier expansion of a plane wave

$$\exp \{-ia \cos \phi\} = \sum_{m=-\infty}^{\infty} (-i)^{|m|} J_{|m|}(a) e^{im\phi}, \quad (31)$$

and letting the magnetic flux and the conical geometry act on it. This involves shifting and rescaling the angular momentum of the modes, as mentioned previously, leading to

$$c_m^{(\delta,\alpha)} := \sqrt{2\pi\alpha} \exp \left\{ -\frac{i\pi}{2\alpha} |m - \delta| \right\}, \quad (32)$$

where the flux parameter has been redefined to be $\delta := -\sigma$ in order to compare the result with earlier work. The stationary state (30) with $c_m = c_m^{(\delta,\alpha)}$ will be denoted $\psi_k^{(\delta,\alpha)}$. Clearly

$$\begin{aligned} \psi_k^{(0,1)}(\rho, \varphi) &= \exp \{ -ik\rho \cos \varphi \} \\ &\equiv \exp \{ -ikX^1 \} \end{aligned} \quad (33)$$

(Note that when $\alpha = 1$, both $\{x^1, x^2\}$ and $\{X^1, X^2\}$ are genuine Cartesian coordinates which coincide.). The stationary states $\psi_k^{(\delta,1)}$ and $\psi_k^{(0,\alpha)}$ have previously been considered in the literature (in [1] and [12, 14] respectively) in the context of scattering. The following section considers the probability fluid (see appendix) associated with $\psi_k^{(\delta,\alpha)}$.

5 Quantum flow

Consider the symmetries of the state $\psi_k^{(\delta,\alpha)}$. By redefining the summation index in (30) it is straightforward to show that

$$\psi_k^{(\delta+n,\alpha)}(\rho, \varphi) = \psi_k^{(\delta,\alpha)}(\rho, \varphi), \quad (34)$$

from which it follows that integer flux parameters are equivalent to zero. Also

$$\psi_k^{(-\delta,\alpha)}(\rho, \varphi) = \psi_k^{(\delta,\alpha)}(\rho, -\varphi) \quad (35)$$

implies that for vanishing flux parameter $\psi_k^{(0,\alpha)}(r, \theta) \equiv \psi_k^{(0,\alpha)}(r, -\theta)$. Thus the quantum flow is symmetric with respect to the x^1 axis and, consequently, no probability from the upper half-plane passes to the lower half-plane and vice versa. In other words the current lines associated with the quantum flow must not cross the x^1 axis, otherwise due to the symmetry, they would intercept on this axis. When the flux parameter is switched on this symmetry is broken, implying that the flow corresponding to a charged particle is sensitive to the direction (up or down) in which the magnetic flux runs. By studying the symmetries (34) and (35), one sees that

$$0 \leq \delta \leq 1/2 \quad (36)$$

covers all possible behaviours of the flow and that $\delta = 1/2$ also yields a flow symmetric with respect to the x^1 axis. Expressions (34) and (35) generalize the known symmetries [26, 2] of the A-B set up to include the presence of a conical singularity.

Considering (30) and (32) it follows the probability density

$$\psi_k^{(\delta,\alpha)} \psi_k^{(\delta,\alpha)*} = \sum_{m,m'=-\infty}^{\infty} \exp \{ i\Theta_{m,m'}^{(\delta,\alpha)}(\varphi) \} J_{|m-\delta|/\alpha}(k\rho) J_{|m'-\delta|/\alpha}(k\rho), \quad (37)$$

where

$$\Theta_{m,m'}^{(\delta,\alpha)}(\varphi) := \frac{1}{\alpha} \left[(|m - \delta| - |m' - \delta|) \frac{\pi}{2} - (m - m') \varphi \right], \quad (38)$$

satisfying $\Theta_{m,m'}^{(\delta,\alpha)} = -\Theta_{m',m}^{(\delta,\alpha)}$. The probability current, when expressed with respect to $\{X^1, X^2\}$, has the familiar polar components on the Euclidean plane (22), from which it follows that

$$\begin{aligned} J_\rho^{(\delta,\alpha)}(\rho, \varphi) &= \frac{\hbar k}{2M} \sum_{m,m'=-\infty}^{\infty} \sin \left\{ \Theta_{m,m'}^{(\delta,\alpha)}(\varphi) \right\} J_{|m-\delta|/\alpha}(k\rho) \\ &\quad \times \left[J_{|m'-\delta|/\alpha-1}(k\rho) - J_{|m'-\delta|/\alpha+1}(k\rho) \right] \end{aligned} \quad (39)$$

and

$$J_\varphi^{(\delta,\alpha)}(\rho, \varphi) = \frac{\hbar}{M\rho} \sum_{m,m'=-\infty}^{\infty} \frac{m' - \delta}{\alpha} \cos \left\{ \Theta_{m,m'}^{(\delta,\alpha)}(\varphi) \right\} J_{|m-\delta|/\alpha}(k\rho) J_{|m'-\delta|/\alpha}(k\rho). \quad (40)$$

In deriving (39), equality (29) has been used.

In the following the quantum flow will be studied when

$$k\rho \ll 1 \quad (41)$$

This amounts to consider the expansion

$$J_\nu(z) = \left(\frac{z}{2}\right)^\nu \left[\frac{1}{\Gamma(1+\nu)} - \frac{1}{\Gamma(2+\nu)} \left(\frac{z}{2}\right)^2 + O(z^4) \right], \quad (42)$$

in (37), (39) and (40), keeping only the terms with small m and m' . For simplicity the cone and the flux tube will be considered separately.

It should be remarked that (41) contrasts with the regime on scattering problems for which $k\rho \gg 1$.

5.1 Conical singularity

Using (38) and (42), it follows from (37) that the first terms of the probability density around a conical singularity are

$$\begin{aligned} \psi_k^{(0,\alpha)} \psi_k^{(0,\alpha)*} &= 1 + \frac{\cos\{\pi/2\alpha\} \cos\{\varphi/\alpha\}}{2^{1/\alpha-2} \Gamma(1+1/\alpha)} (k\rho)^{1/\alpha} - \frac{1}{2} (k\rho)^2 \\ &\quad + \frac{\alpha^2}{2^{2/\alpha-1}} \left[\frac{1 + \cos\{2\varphi/\alpha\}}{\Gamma^2(1/\alpha)} + \frac{\cos\{\pi/\alpha\} \cos\{2\varphi/\alpha\}}{\alpha \Gamma(2/\alpha)} \right] (k\rho)^{2/\alpha}, \end{aligned} \quad (43)$$

where all terms of the order of $(k\rho)^\lambda$, with $\lambda \leq 2$ and $1/2 < \alpha < 3/2$, have been considered. When $\alpha = 1$ the corresponding (non zeroth) powers of $k\rho$ in (43) cancel out as they should be since in the absence of the conical singularity (and of magnetic flux) the probing state becomes a plane wave [see (33)].

In studying the probability density (43), one may be led to conclude that the configuration space of a particle in the state $\psi_k^{(0,\alpha)}$ is simply connected, since $\psi_k^{(0,\alpha)}\psi_k^{(0,\alpha)*}$ does not vanish at the conical singularity (i.e. in the limit $k\rho \rightarrow 0$). However, the following considerations may lead to a different interpretation. A way of preventing a particle of getting inside a disc centered at the origin is to impose boundary conditions such that the radial component of the probability current vanishes on the border of the disc (and this may be implemented without requiring that the wave function itself vanishes at the border). Thus no probability leaks into the hole and the current lines surround the disc without crossing it. This is a non simply connected configuration space. When the disc degenerates to a point at the origin, this picture does not change. At the origin, which is now border of the disc, the radial probability current vanishes. It is reasonable to say that the configuration space of this particle is $R^2 - \{0\}$, although the probability density may be non vanishing at the origin. If this interpretation is adopted, it follows that before making any statement about connectivity of the configuration space of a particle on the cone, one should also study the probability current at the singularity.

Before determining the behaviour of the probability current at the conical singularity, consider its corresponding quantum potential (54). The term containing $(k\rho)^{1/\alpha}$ in (43) satisfies the Laplace equation and, consequently, does not give any information about the quantum potential (that is the reason why higher order corrections in (43) were considered). For $1/2 < \alpha < 3/2$ it follows from (54) and (43) that the quantum potential near the conical singularity is approximately given by

$$V_\alpha(\rho) = -\frac{(\hbar k)^2}{2M} \frac{(k\rho/2)^{2/\alpha-2}}{\Gamma^2[1/\alpha]}, \quad (44)$$

where an unimportant constant has been dropped. The fact that (44) is not a constant when the conical singularity is present ($\alpha \neq 1$) constitutes a genuine quantum mechanical effect (a geometrical Aharonov-Bohm effect). Far away from the conical singularity, for positive X^1 , the state $\psi^{(0,\alpha < 1/2)}$ behaves approximately as the plane wave (33) [12, 14]. Consequently, in terms of $\{X^1, X^2\}$, the current lines of the quantum flow are approximately straight lines parallel to the X^1 axis, running to the left. At this stage, the quantum flow coincides with a flow of classical particles (see section 3). As the singularity is approached, the two flows depart from each other. Near the conical singularity they differ radically - by differentiating the quantum potential (44), it follows that the current lines are scattered away from the conical singularity when $\alpha < 1$ and bent towards it when $\alpha > 1$, whereas the classical particles experience no force (in the $\{X^1, X^2\}$ frame). When $\alpha = 1$, the quantum potential (44) becomes constant and the classical and quantum flows coincide everywhere, as they must.

After this rather qualitative analysis, the probability current will now be determined near the conical singularity. By proceeding as one did to obtain (43), from (39) and (40) it follows that

$$J_\rho^{(0,\alpha)}(\rho, \varphi) = -\frac{\hbar k}{M} \left(\frac{k\rho}{2}\right)^{1/\alpha-1} \left[\frac{\sin\{\pi/2\alpha\} \cos\{\varphi/\alpha\}}{\Gamma(1/\alpha)} + \frac{\sin\{\pi/\alpha\} \cos\{2\varphi/\alpha\}}{2^{1/\alpha}\Gamma(2/\alpha)} (k\rho)^{1/\alpha} \right] \quad (45)$$

and

$$J_{\varphi}^{(0,\alpha)}(\rho, \varphi) = \frac{\hbar k}{M} \left(\frac{k\rho}{2} \right)^{1/\alpha-1} \left[\frac{\sin\{\pi/2\alpha\} \sin\{\varphi/\alpha\}}{\Gamma(1/\alpha)} + \frac{\sin\{\pi/\alpha\} \sin\{2\varphi/\alpha\}}{2^{1/\alpha}\Gamma(2/\alpha)} (k\rho)^{1/\alpha} \right], \quad (46)$$

where terms $O[(k\rho)^2]$ and $O[(k\rho)^{2/\alpha}]$ have been omitted for $\alpha \leq 1$ or $\alpha > 1$, respectively. When $1/\alpha$ is even, one sees that the expressions (45) and (46) vanish, which is consistent with the fact that the stationary state $\psi_k^{(0,1/2n)}$ is a real function [14]. This effect becomes more intuitive by recalling that for even $1/\alpha$ classical particles are scattered backwards, and then the scattered classical flow cancels the incident one, resulting in a vanishing *net* classical flow. Clearly when $\alpha = 1$ (45) and (46) imply that $J_{\rho}^{(0,1)}(\rho, \varphi) = -(\hbar k/M) \cos \varphi$ and $J_{\varphi}^{(0,1)}(\rho, \varphi) = (\hbar k/M) \sin \varphi$, which are the polar components of the plane wave probability current,

$$J^{(0,1)}(\rho, \varphi) = -\frac{\hbar k}{M} \mathbf{e}_1 \quad (47)$$

$[\mathbf{e}_1 := (1, 0)]$ as expected. From (45) and (46), one sees that in the limit $\rho \rightarrow 0$ the probability current either vanishes or diverges for $\alpha < 1$ and $\alpha > 1$, respectively. Note that although $J_{\rho}^{(0,\alpha>1)}$ diverges as $\rho \rightarrow 0$, the r.h.s. of (21) vanishes, which is not surprising since this was the criterion for choosing the stationary states. The fact that for $\alpha < 1$ the quantum flow avoids the conical singularity suggests that the corresponding configuration space is non simply connected (and vice versa for $\alpha \geq 1$), as discussed previously. At this point it should be remarked that according to the authors of [16], if $\psi \neq 0$ at the conical singularity, the configuration space is simply connected and, consequently, two identical particles on the plane ($\alpha = 1/2$) in the state ψ “collide”. The analysis of the quantum flow above seems to suggest that this may be not the case.

Due to the presence of the wedge in the singular Cartesian coordinates $\{X^1, X^2\}$, for some purposes it is more convenient to describe the flow in terms of the embedded Cartesian coordinates $\{x^1, x^2\}$. By performing the coordinate transformation $X^i \rightarrow x^i$ it is straightforward to show that, in the $\{x^1, x^2\}$ frame, probability current is given by $\mathbf{j} = j_r \mathbf{e}_r + j_{\theta} \mathbf{e}_{\theta}$, with $j_r = \alpha J_{\rho}$ and $j_{\theta} = J_{\varphi}$. (Note that the wave function and \mathbf{j} satisfy the usual Cartesian form of the continuity equation.) Then, keeping only the leading contribution in (45) and (46), one finds

$$\mathbf{j}^{(0,\alpha)}(r, \theta) = -\frac{\hbar k}{M} \left(\frac{kr}{2\alpha} \right)^{1/\alpha-1} \frac{\sin\{\pi/2\alpha\}}{\Gamma(1/\alpha)} [\mathbf{e}_1 + (\alpha - 1) \cos \theta \mathbf{e}_r], \quad (48)$$

where the features mentioned above may easily be verified. For example setting $\alpha = 1$ in (48) reproduces (47).

Figures 5, 6 and 7 show the current lines associated with $\mathbf{j}^{(0,\alpha)}$ for $\alpha < 1$, $\alpha = 1$ and $\alpha > 1$. They have been obtained by plotting the numerical integration of the equations resulting by equating $d\mathbf{x}/d\lambda$ to the term between brackets in (48),

$$\frac{dx^1}{d\lambda} = 1 + (\alpha - 1) \frac{(x^1)^2}{(x^1)^2 + (x^2)^2} \quad \frac{dx^2}{d\lambda} = (\alpha - 1) \frac{x^1 x^2}{(x^1)^2 + (x^2)^2},$$

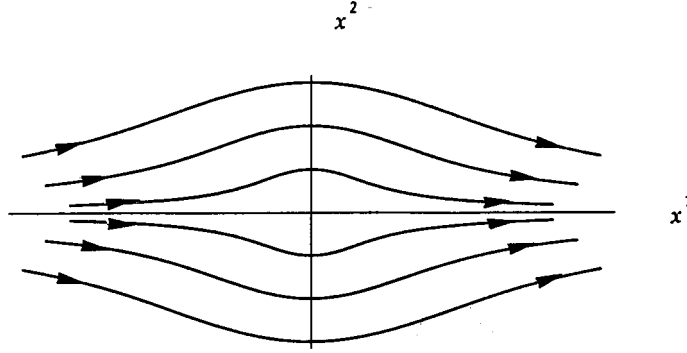


Figure 5: Quantum flow when $\alpha < 1$.

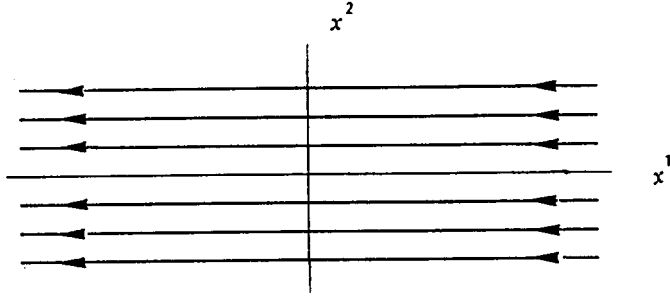


Figure 6: Quantum flow when $\alpha = 1$.

where λ is an arbitrary parameter.

At $\theta = 0, \pm\pi/2$ and π the flow runs parallel to the x^1 axis, as may be seen from (48). As the direction of $\mathbf{j}^{(0,\alpha)}$ in (48) for a given α is determined by θ only, the current lines are parallel to each other (a feature shared with the classical flow). However this is true only very close to the singularity, where the subleading contributions in (45) and (46) are not relevant. Apart from diverging at the conical singularity for $\alpha > 1$, the probability current is smooth everywhere.

Consider more carefully the factor $f(r, \mathcal{D}) := (kr)^{1/\alpha-1}$ in (48). For an infinitesimal $\epsilon > 0$, $f(0, 0 + \epsilon) = 0$, $f(0, 0) = 1$ and $f(0, 0 - \epsilon) = \infty$. This discontinuity makes the behavior of the quantum flow on the Euclidean plane change abruptly in the presence of a tiny deficit angle. No such effect exists at classical level, where the velocity of the particles varies smoothly with the deficit angle. This effect is less suprising by recalling that even a tiny deficit angle ϵ corresponds to a delta function curvature which “pierces” the configuration space.

An unsuspected relationship between the winding number of classical orbits and the quantum flow arises when studying the direction of the latter [left or right, with the flow

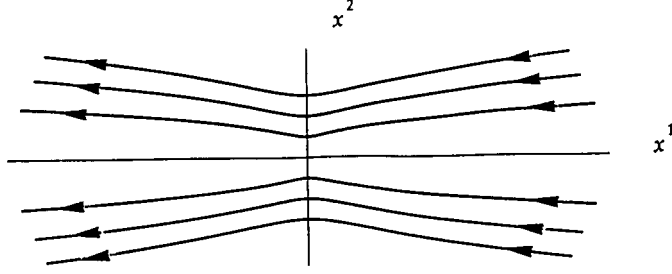


Figure 7: Quantum flow when $\alpha > 1$.

(47) running to the left]. Such direction is determined by the factor $\sin\{\pi/2\alpha\}$ in (48). For $\alpha > 1/2$ the quantum flow always runs to the left, and the classical particles are scattered without winding around the conical singularity. For $\alpha = 1/2$ (classical backward scattering) the quantum flow stops and reverses its direction for $\alpha < 1/2$, with the classical particles winding once around the conical singularity. It continues to run to the right until one decreases α to $1/4$ when another classical backward scattering takes place with another interruption of the flow. By further decreasing α , the quantum flow starts to run to the left, while the classical particles wind twice around the conical singularity. Generically, the direction of the quantum flow is controlled by the winding number w defined in (10) - the quantum flow runs to the left for even w and to the right for odd w .

From Fig. 5, one sees that for $\alpha < 1$ the quantum flow negotiates the conical singularity in a manner similar to the one in which a low velocity fluid negotiates a cylinder. This analogy may be taken as an evidence that the configuration space is not simply connected when $\alpha < 1$, as was suggested above. Note that there are no vortices present anywhere since the magnetic flux is switched off [observe (58)].

5.2 Flux tube

Now consider non-vanishing magnetic flux in the absence of a conical singularity. The analog of (43) is

$$\begin{aligned} \psi_k^{(\delta,1)} \psi_k^{(\delta,1)*} &= \frac{1}{2^{2\delta} \Gamma^2(1+\delta)} (k\rho)^{2\delta} + \frac{\sin\{\varphi + \delta\pi\}}{\Gamma(1+\delta)\Gamma(2-\delta)} k\rho \\ &\quad - \frac{\sin\varphi}{2^{2\delta} \Gamma(1+\delta)\Gamma(2+\delta)} (k\rho)^{1+2\delta} + \frac{1}{2^{2-2\delta} \Gamma^2(2-\delta)} (k\rho)^{2-2\delta}, \end{aligned} \quad (49)$$

where all terms of order $(k\rho)^\lambda$ were taken into account, with $\lambda \leq 1$, and (36) was considered. Expression (49) agrees with the one in [2] where a slightly different method has been used. For $\delta = 0$ (49) reduces to unity up to a $(k\rho)^2$ term, which would be canceled if higher

powers of $k\rho$ in (49) had been kept. For non vanishing flux parameter, the probability density vanishes at the flux tube ($\rho = 0$) and the corresponding configuration space is non simply connected. The expression for the quantum potential corresponding to (49) will not be given here. Instead a study of the probability current itself is carried out in the following.

As in the case of the conical singularity, (39) and (40) may be used to obtain $J_\rho(\rho, \varphi)$ and $J_\varphi(\rho, \varphi)$. The expressions which correspond to (45) and (46) have previously been found in [2] (see also [26]). The study will be limited to the case where the flux parameter is very small, viz. $\delta \ll 1$. In so doing, $\mathbf{J} = J_\rho \mathbf{e}_\rho + J_\varphi \mathbf{e}_\varphi$ reads approximately

$$\mathbf{J}^{(\delta,1)}(\rho, \varphi) = \frac{\hbar k}{M} \left[\mathbf{e}_\delta - \frac{\delta}{k\rho} \mathbf{e}_\varphi \right], \quad (50)$$

where \mathbf{e}_δ is the unit vector \mathbf{e}_ρ evaluated at $\varphi = \pi(1 - \delta/2)$. When $\delta = 0$, (50) reduces to (47), as should be. Clearly \mathbf{J} vanishes when $\mathbf{e}_\varphi = \mathbf{e}_\delta$ and $k\rho = \delta$, so that

$$(\rho, \varphi) = (\delta/k, \pi(1 - \delta)/2). \quad (51)$$

It is also clear from (50) that the quantum flow (under the action of the corresponding quantum potential) circulates around the origin when it is close to the origin [26]. It turns out that (51) is a stagnation point and that there is a vortex around the flux tube, which was expected by observing (58). In Fig. 8 the numerical solution of

$$\frac{dx^1}{d\lambda} = -1 + (\delta/k) \frac{x^2}{(x^1)^2 + (x^2)^2} \quad \frac{dx^2}{d\lambda} = -(\delta/k) \frac{x^1}{(x^1)^2 + (x^2)^2},$$

is plotted, showing the main features of the quantum flow near the flux tube. It is in agreement with [2] where the analytical expression for the current lines was given.

One sees from (50) that, as with the conical singularity, the delta function magnetic field at the origin imparts a discontinuous change in the quantum flow of a charged particle. Any tiny amount of magnetic flux changes the topology of the current lines (open lines become loops) near the origin. From Fig. 8 one sees that, as previously mentioned, the presence of the magnetic flux breaks the symmetry with respect the X^1 axis. Notice that, as the distance from the origin increases (still for $k\rho \ll 1$), the flow gradually approaches that of a plane wave (47), unlike the effect caused by the conical singularity. An important distinction between the effects caused by the conical singularity and the magnetic flux is that the latter only affects charged particles ($\delta \neq 0$), whereas the former affects all particles, indifferently. This fact may be seen as a manifestation of the equivalence principle - geometrical Aharonov-Bohm effects due to a conical singularity do not depend on any particle attribute.

6 Summary

Summarizing, it was shown that the motion of a particle on a flux cone can be regarded as a motion under the action of an angular-momentum dependent central force. Due to local

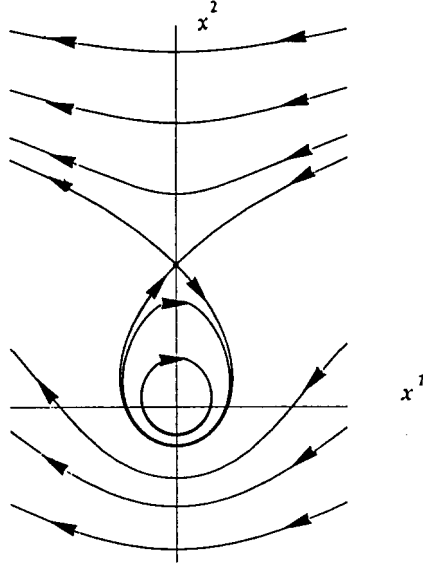


Figure 8: Quantum flow around a flux tube.

flatness, quantization was implemented along usual procedures in flat space. By studying the probability fluid corresponding to a particular stationary state (“plane wave” on a flux cone), new effects were found. For example it was shown that the winding number of classical orbits controls the direction of the quantum flow on a cone. Classical flow (which is nearly trivial) and quantum flow were shown to depart from each other near the singularity due to the presence of a non vanishing quantum force. For the case of a conical singularity, the corresponding quantum potential was determined and analyzed. The issue of connectivity of the configuration space was treated and some interpretations were proposed.

Other boundary conditions at the singularity (those considered in [15, 16]) may lead to new effects. Another interesting extension of this work would be to consider relativistic particles. The use of this approach in the study of quantum flow in the context of other geometries and topologies would be worthwhile, particularly in geometries with horizons.

A Hydrodynamical approach to quantum mechanics

The analogies between quantum mechanics and fluid dynamics do not stop at a continuity equation which expresses local conservation of probability. The Schrödinger equation can be rephrased as a set of hydrodynamical equations (see [2] and references therein). In order to derive them consider a particle with charge e moving in the Euclidean space (the generalization to arbitrary backgrounds is straightforward) under the action of an electromagnetic field (\mathbf{E}, \mathbf{B}) with corresponding potentials (ϕ, \mathbf{A}) . The Hamiltonian operator is

then given by

$$H = \frac{1}{2M} \left(-i\hbar\nabla - \frac{e}{c}\mathbf{A} \right)^2 + e\phi. \quad (52)$$

Now one rewrites the solution ψ for the corresponding Schrödinger equation as

$$\psi(t, \mathbf{r}) = \varrho(t, \mathbf{r}) e^{i\chi(t, \mathbf{r})}.$$

The real part of the Schrödinger equation reads

$$\hbar \frac{\partial \chi}{\partial t} + \frac{\hbar^2}{2M} \left[\nabla \chi - \frac{e}{c\hbar} \mathbf{A} \right]^2 + e\phi + V = 0, \quad (53)$$

where

$$\begin{aligned} V(t, \mathbf{r}) &:= -\frac{\hbar^2}{2M} \frac{\nabla^2 \varrho}{\varrho} \\ &\equiv -\frac{\hbar^2}{2M} \frac{\nabla^2 (\psi\psi^*)^{1/2}}{(\psi\psi^*)^{1/2}}. \end{aligned} \quad (54)$$

The imaginary part reads

$$\frac{\partial \varrho^2}{\partial t} + \nabla \cdot (\varrho^2 \mathbf{v}) = 0 \quad (55)$$

with

$$\mathbf{v} := [\hbar \nabla \chi - e\mathbf{A}/c]/M, \quad (56)$$

leading to the constraint

$$\nabla \times \mathbf{v} = -\frac{e}{Mc} \mathbf{B}. \quad (57)$$

Now one sees that $\varrho^2 \mathbf{v}$ is the probability current and therefore (55) is just the continuity equation. Note that by integrating (57) along a closed loop it follows

$$\oint \mathbf{v} \cdot d\mathbf{l} = -\frac{e\Phi}{Mc}, \quad (58)$$

where Φ is the magnetic flux enclosed by the loop.

The last step is to apply ∇ on (53), after which one is left with a set of equations of motion for a fluid of density ϱ^2 and velocity \mathbf{v} ,

$$\begin{aligned} M \frac{d}{dt} \mathbf{v}(t, \mathbf{r}) &\equiv M \left[\frac{\partial \mathbf{v}}{\partial t} + (\mathbf{v} \cdot \nabla) \mathbf{v} \right] \\ &= e\mathbf{E} + \frac{e}{c} \mathbf{v} \times \mathbf{B} - \nabla V. \end{aligned} \quad (59)$$

Thus, the wave like Schrödinger equation [where the function to be determined is ψ for a given configuration of potentials (ϕ, \mathbf{A})] has been replaced by the hydrodynamical equations (55) and (59) with the constraint (57) [where the functions to be determined are (ϱ, \mathbf{v}) for a

given configuration of electromagnetic field (\mathbf{E}, \mathbf{B}) . These equations govern the behaviour of the quantum flow.

Whereas the Schrödinger equation is more appropriate to study wave like features of quantum mechanics, the hydrodynamical equations are more appropriate to study particle like features. To see this, assume that the quantum force $-\nabla V$ in (59) is negligible when compared with the Lorentz force (and other forces that one might have considered). In this “classical limit”, (59) reduces to the equations of motion for a flow of non-interacting classical particles. Note that (53) is the corresponding Hamilton-Jacobi equation where the action is identified with $\hbar\chi$. It is clear that the quantum potential V represents the departure from the classical motion. In regions where the quantum potential is relevant, the classical and quantum flow may differ considerably from each other. For example, in a region of vanishing field strengths the motion of the classical flow is trivial, since the Lorentz force vanishes there. The motion of the quantum flow, on the other hand, may be quite elaborate due to the presence of the quantum force $-\nabla V$ in (59). A non vanishing quantum force is the essence of Aharonov-Bohm like effects.

Acknowledgements. The author is grateful to George Matsas for reviewing the manuscript and for clarifying discussions.

References

- [1] Aharonov, Y. and Bohm, D., Phys. Rev. **115**, 485, (1959)
- [2] Olariu, S. and Popescu, I. I., Rev. Mod. Phys. **57**, 339, (1985)
- [3] Marder, L., Proc. Roy. Soc., A **252**, 45, (1959)
- [4] Staruszkiewicz, A., Acta. Phys. Polon. **24**, 734, (1963)
- [5] Dowker, J. S., Nuovo Cimento **52** B, 129, (1967)
- [6] Linet, B., Phys. Rev. D **33**, 1833, (1986)
- [7] Smith, A. G. In “Proc. of the Workshop on The formation and evolution of cosmic strings”, Gibbons, G. W., Hawking, S. W. and Vachaspati, T. (eds.), Cambridge, 1989. Cambridge University Press, Cambridge, (1990).
- [8] Vilenkin, A. and Shellard, E. P. S., “Cosmic Strings and Other Topological Defects”, Cambridge University Press, Cambridge, (1994).
- [9] Dowker, J. S., J. Phys. A **10**, 115, (1977); Phys. Rev. D **18**, 1856, (1978)
- [10] Helliwell, T. M. and Konkowski, D. A., Phys. Rev. D **34**, 1918, (1986); Linet, B., Phys. Rev. D **35**, 536, (1987); Frolov, V. P. and Serebriany, E. M., Phys. Rev. D **35**, 3779, (1987); Dowker, J. S., Phys. Rev. D **36**, 3095, (1987); Dowker, J. S., Phys. Rev. D **36**, 3742, (1987)

- [11] Zerbini, S., Cognola, G. and Vanzo, L., Phys. Rev. D **54**, 2699, (1996)
- [12] Lancaster, D., Ph.D. thesis, Stanford University, (1984); Phys. Rev. D **42**, 2678, (1990)
- [13] 't Hooft, G., Commun. Math. Phys. **117**, 685, (1988)
- [14] Deser, S. and Jackiw, R., Commun. Math. Phys. **118**, 495, (1988)
- [15] Kay, B. S. and Studer, U. M., Commun. Math. Phys. **139**, 103, (1991)
- [16] Bourdeau, M. and Sorkin, R. D., Phys. Rev. D **45**, 687, (1992)
- [17] Sokolov, D. D. and Starobinskii, A. A., Sov. Phys. Dolk. **22**, 312, (1977)
- [18] Deser, S., Jackiw, R. and 't Hooft, G., Ann. Phys. **152**, 220, (1984)
- [19] Clément, G., Intern. Jour. Theor. Phys. **24**, 267, (1985)
- [20] Jackiw, R. and Redlich, A. N., Phys. Rev. Lett. **50**, 555, (1983)
- [21] Felsager, B., “Geometry, particles and fields”, Odense University Press, Odense, (1981).
- [22] Bezerra, V. B., J. Math. Phys. **30**, 2895, (1989)
- [23] Dirac, P. A. M., Proc. R. Soc. London A **133**, 60, (1931)
- [24] Gerbert, P. S. and Jackiw, R., Commun. Math. Phys. **124**, 229, (1989)
- [25] Gerbert, P. S., Nucl. Phys. B **346**, 440, (1990)
- [26] Berry, M. V., Chambers, R. G., Large, M. G., Upstill, C. and Walmsley, J. C., Eur. J. Phys. **1**, 154, (1980)